

## Article

# Validation of a Method to Select A Priori the Number of Typical Days for Energy System Optimisation Models <sup>†</sup>

Paolo Thiran <sup>\*</sup>, Hervé Jeanmart  and Francesco Contino Institute of Mechanics, Materials and Civil Engineering, Université Catholique de Louvain,  
1348 Louvain-la-Neuve, Belgium<sup>\*</sup> Correspondence: paolo.thiran@uclouvain.be<sup>†</sup> SDEWES 2022—The 17th Conference on Sustainable Development of Energy, Water and Environment Systems,  
Paphos, Cyprus, 6–10 November 2022.

**Abstract:** Studying a large number of scenarios is necessary to consider the uncertainty inherent to the energy transition. In addition, the integration of intermittent renewable energy sources requires complex energy system models. Typical days clustering is a commonly used technique to ensure the computational tractability of energy system optimisation models, while keeping an hourly time step. Its capability to accurately approximate the full-year time series with a reduced number of days has been demonstrated (i.e., *a priori* evaluation). However, its impact on the results of the energy system model (i.e., *a posteriori* evaluation) is rarely studied and was never studied on a multi-regional whole-energy system. To address this issue, the multi-regional whole-energy system optimisation model, EnergyScope Multi-Cells, is used to optimise the design and operation of multiple interconnected regions. It is applied to nine diverse cases with different numbers of typical days. A bottom-up *a posteriori* metric, the design error, is developed and analysed in these cases to find trade-offs between the accuracy and the computational cost of the model. Using 10 typical days divides the computational time by 8.6 to 23.8, according to the case, and ensures a design error below 17%. In all cases studied, the time series error is a good prediction of the design error. Hence, this *a priori* metric can be used to select the number of typical days for a new case study without running the energy system optimisation model.



**Citation:** Thiran, P.; Jeanmart, H.; Contino, F. Validation of a Method to Select A Priori the Number of Typical Days for Energy System Optimisation Models. *Energies* **2023**, *16*, 2772. <https://doi.org/10.3390/en16062772>

Academic Editors: Francesco Calise, Neven Duić, Poul Alberg Østergaard, Qiuwang Wang and Maria da Graça Carvalho

Received: 14 January 2023

Revised: 20 February 2023

Accepted: 3 March 2023

Published: 16 March 2023



**Copyright:** © 2023 by the authors. Licensee MDPI, Basel, Switzerland. This article is an open access article distributed under the terms and conditions of the Creative Commons Attribution (CC BY) license (<https://creativecommons.org/licenses/by/4.0/>).

**Keywords:** energy system modelling; temporal aggregation; typical days; clustering; whole-energy system; sector-coupling; energyscope; energy system optimisation model

## 1. Introduction

Optimal planning of the integration of weather-dependent renewable energy sources (RES) requires complex energy system models [1]. A whole-energy system approach is necessary to consider all the levers to compensate for the intermittency of these variable renewable energy sources (VRES) [2]. In addition, they must include an hourly variation of the production and demand [3]. As these models forecast energy systems over several decades, it induces high uncertainties in input data [4]. Hence, to give a meaningful view of the energy transition options, a global sensitivity analysis must be performed. For instance, Rixhon et al. [5] needed 1595 model evaluations for a regional whole-energy system, even though they used a state-of-the-art global sensitivity analysis approach. To limit the computational burden of these complex models, several performance enhancement techniques have been developed [6]. They are solver-based or model-based. The first category consists of selecting the best modelling approach and solver. In general, for complex energy system optimisation models (ESOMs), a linear or integer optimisation problem is formulated [7]. The model-based category includes the following: (i) exact mathematical decomposition [8–10]; (ii) heuristic decomposition [11–13]; and (iii) model reduction techniques [14,15]. The two types of decomposition techniques take advantage of the mathematical structure of the problem to separate it into linked sub-problems. They are less often

used than model reduction for integrated energy system models because of the size, complexity and linked nature of the optimisation problem [6]. The model reduction techniques consist of aggregating the data to simplify the model evaluation. This aggregation must be performed wisely to improve performance while maintaining correct accuracy. It can be performed on a temporal level [16–19], a spatial level [20–25] or a technological level [26–28]. Temporal aggregation is the most commonly used and regroups a set of different techniques: from the simple down-sampling that can provide a reduction in computational time of 80% but loses a significant part of the dynamic of VRES [29] to the more complex typical days (TDs) clustering which relies on recurrent patterns in VRES production and variable demands. This type of technique has become the most studied temporal aggregation technique in the last few years [16]. Different TDs selection approaches have been applied and compared: heuristics [29–32], random selection [30], k-means clustering [33–38], k-medoid clustering [33–35,39–41], hierarchical clustering [30,33,34,37,42,43], chronological clustering [37,44] and hybrid methods [29,30]. In addition, some authors have underlined the importance of considering extreme days [29,45,46] and inter-annual variability [29,47] in the clustering of TDs. To evaluate the selected TDs and choose the “best” number of TDs, a diversity of evaluation metrics is proposed in the literature. Most papers look at *a priori* metrics, that is, without running the energy system model. The most common ones are the error on the time series and on their duration curve [18,37,39,42,48]. Some also consider the error in the correlation between time series [42]. However, the impact on the accuracy of the energy system optimisation results is rarely studied [6]. When it is, most authors limit themselves to evaluating the error on the objective function [18,34,36,42,44,48,49]. In this objective function, some parts of the system, very insensitive to the temporal resolution, hide errors on other key elements. Hence, as it is shown later in this study, analysing the objective function tends to underestimate the impact of the number of TDs. Some studies consider, in addition, summarized results of their optimisation, such as power generators, storage assets and transmission lines [6,29,37,38,50]. However, in all these cases, the model focuses on the electricity sector, and their method is hard to extend to a whole-energy system approach, because a multitude of different technologies, resources and energy fluxes (e.g., electricity, heat, synthetic molecules) are present and cannot be compared directly (e.g., 1 GWh of low-temperature heat does not have the same value as 1 GWh of synthetic methane). Limpens et al. [41] proposed a first approach for whole-energy system models. They chose 12 TDs with a k-medoid clustering algorithm. This leads, in their case, in the Swiss energy system, to an under-sizing of 74.8% of seasonal thermal storage. Their work cannot be directly extended to a multi-regional whole-energy system. Indeed, considering multi-regional cases multiplies the number of time series to consider and complexifies the TDs clustering. Furthermore, it is not possible to predict *a priori* if the results observed in the 1-region Swiss case extend to multi-regional cases. To the best authors’ knowledge, there exists no method suitable to evaluate the impact on a multi-regional whole-energy system. Furthermore, no study linked the *a priori* evaluation of TDs clustering and the impact on the energy system results.

The objective of this paper is to fill these two gaps: (i) developing an error metric to evaluate the sensitivity of energy system results to the number of TDs, suitable for any ESOM and any case study; (ii) comparing this *a posteriori* metric with the classical *a priori* metrics to find out which one of these *a priori* metrics gives a good estimation of the impact of the number of TDs on the energy system results. To carry this out, the methodology is developed and tested on nine cases with different typologies and numbers of regions. For each case, the clustering of TDs is evaluated in a classical way by computing the error on the time series, on their duration curve and on the correlation between the time series. Then, the open-source, multi-regional whole-energy system model, EnergyScope Multi-Cells [51–53], is applied for different numbers of TDs with a 90% reduction in direct CO<sub>2</sub> emissions. Its sensitivity to the number of TDs is studied, and a design error (*DE*) is developed, based on the sizing of the technologies and the use of primary energy resources.

A strong correlation between the time series error (*TSE*) and the design error (*DE*) is underlined, and a generalized method is proposed for any new case studies.

The paper is structured as follows. First, Section 2 explains the ESOM used, the TDs clustering algorithm, how the TDs are integrated into the model formulation and how their impact is evaluated *a priori* and *a posteriori*. Then, Section 3 presents and motivates the studied cases. Afterwards, Section 4 presents, compares and discusses the *a priori* and *a posteriori* evaluation of TDs clustering. From this, an *a priori* method to choose the number of TDs is proposed. Finally, Section 5 underlines the key findings, their limitations and how they fill the gap in the literature.

## 2. Methods

This section presents the energy system optimisation model (ESOM), the TDs clustering algorithm and how the TDs are included in the model. Then, the methods to evaluate this clustering of TDs and its impact on the energy system results are explained.

### 2.1. Energy System Optimisation Model

A multi-regional whole-energy system model, EnergyScope Multi-Cells, is used. It is a linear programming model optimising the annualised total cost of the system under several constraints: greenhouse gases emissions reduction, power balance for each energy carrier, exchanges between cells, storage level, availability of resources, etc. This model is built as an extension of the open-source model EnergyScope TD [41]. The validity of both the original model [5,54–61] and the extension [51,62,63] was verified in previous studies.

This extension adds the possibility of representing different regions, also called cells. Each cell is considered as one node where the energy balance for each energy carrier is ensured for all time steps, and it is capable of exchanging different energy carriers with other cells: electricity, methane, ammonia, methanol, woody biomass and waste. Both the quantity exchanged and the interconnector sizes, or the freight needed to transport these resources, are optimised by the model. In each region, the model considers 9 different end-use demands: electricity, space heating and hot water, space cooling, passenger and freight mobility, high-temperature heat and process cooling for the industry and non-energy demand. To supply these demands, it has access to 19 different energy resources (e.g., wind, sun, fossils, biomass) either extracted locally or imported and can choose among 120 different technologies to convert these resources into the demands. The main outputs of the model are the sizing and the hourly operation of the technologies as well as the use of primary energy resources and the exchanges between regions. The input data, code and Supplementary material of the model can be found online [52,53].

### 2.2. Typical Days Clustering Method

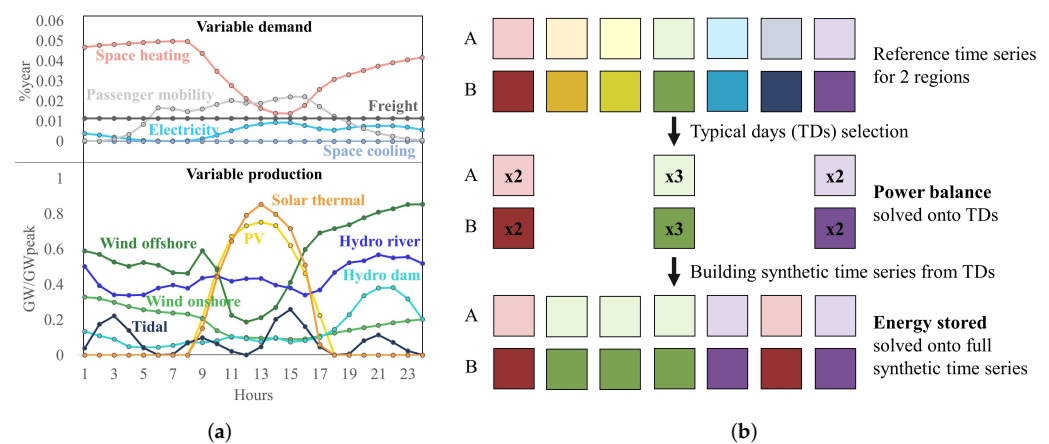
As illustrated in Figure 1a, a multi-regional whole-energy system approach induces the need to consider several time-dependent attributes for each region: electricity demand, heating demand, cooling demand, mobility demand and weather-dependent RES (i.e., 7 resources per cell in this model). Each of them is represented by an hourly time series, increasing the complexity of the clustering. For variable demands, the time series represent the share at each hour of the total demand over the year (%*year*). For weather-dependent RES, the time series give the production per peak unit installed ( $GW/GW_{peak}$ ).

Figure 1b presents the TD approach implemented to enhance the performance of the multi-regional whole-energy system optimisation model. It is a simplified conceptual illustration: the selection of 3 TDs to represent a week for 2 different regions (A and B). Each region is represented by a row and each day by a square of a different colour. Figure 1a is a zoom on one day to present the time series considered. Limpens et al. [41] have compared several algorithms for this typology of problem and have chosen a k-medoid algorithm developed by Dominguez-Muñoz et al. [39]. It has a simple mixed-integer programming formulation, fast convergence and low error on both time series and duration curves. In this study, we will use this algorithm as such. However, based on the approach developed in the

following sections, this algorithm could be fine-tuned and compared to other algorithms in the literature. In this algorithm, the days are grouped into clusters to minimise the intra-cluster distance, and the medoid of the cluster is taken as TD. The distance between 2 different days is defined as follows:

$$Dist(i, j) = \sum_{a \in A} \omega_a \sum_{h=1}^{24} |ts(a, h, i) - ts(a, h, j)| \quad (1)$$

To compute the distance ( $Dist$ ) between 2 days ( $i$  and  $j$ ), the L1 norms between each hour ( $h$ ) for the time series ( $ts$ ) representing each attribute ( $a$ ) are summed over the 24 h of the day. This gives the distance for each attribute. Then, a weighted sum of these distances is computed. The number of attributes corresponds to the number of time series considered multiplied by the number of regions studied. The weights ( $\omega_a$ ) are important hyperparameters of the clustering algorithm. Hence, the metrics developed in this study could help refine them. As a first approach, the weights are defined to reflect the importance of each attribute in the energy system: (i) only the attributes with different time series between the different days are considered. For instance, in this model, the freight is considered constant over the entire year, and the public mobility has the same time series for each day of the year. Hence, they are not considered for the TDs clustering; (ii) the sum of the weights of the different attributes is equal to 1 with 0.5 for the attributes defining the variable demand and 0.5 for the attributes defining the variable production; (iii) among the variable demands, the weight is split according to the total demand over the year, considering Carnot coefficient of performance to scale space heating and space cooling demands; and (iv) among the variable productions, the weight is split according to their yearly production at full potential deployment.



**Figure 1.** Conceptual illustration of the typical day's integration into a multi-regional whole-energy system model: (a) Illustration of the time series considered for one day and one region. (b) Simplified situation where 3 typical days (TDs) are used to represent a week for 2 different regions (A and B). Each line represents one region, and each colour one day.

The clustering algorithm selects the same days as TDs for all the regions (Figure 1b, second step). As these days have different time series in the different regions, it ensures the temporal synchronicity of the different regions while considering the spatial disparity of demands and productions. Hence, the TDs selection considers both the intra- and inter-regional relations among the time series. In addition to the clustering algorithm, preprocessing and postprocessing of the time series are performed. During the preprocessing, the time series are normalised such that their sum over the year is equal to 1, while in the postprocessing, the time series of the TDs are rescaled to preserve the average value over the year.

In the optimisation model, the power balance equations are solved on the chosen TDs (Figure 1b, second step). This reduces the number of variables and constraints. To consider longer-term storage, the storage level equations are solved over the synthetic time series. These synthetic time series are built by replacing each day with its TD (Figure 1b, third step). This method was introduced by Gabrielli et al. [38]. In EnergyScope Multi-Cells, the concept illustrated in Figure 1 is applied to the entire year.

### 2.3. Sensitivity to the Number of Typical Days

This subsection presents the methods to assess the quality of the representation with TDs and its impact on the energy system results. Therefore, the model is run with different numbers of TDs from 2 to 365: (i) from 2 to 62 with steps of 2; (ii) from 62 to 110 with steps of 4; (iii) from 120 to 180 with steps of 20; (iv) 365. At low numbers of TDs, more model evaluations are performed because more changes occur. The case with the full-year (i.e., 365 TDs) is the reference one. The error due to the number of TDs is assessed *a priori*, i.e., without running the energy system model, and *a posteriori*, i.e., from the energy system optimisation results. Then, the correlation between the metric developed on energy system results and the *a priori* metrics is studied. This analysis gives the best *a priori* metric for the selection of the number of TDs for a new case study.

#### 2.3.1. A Priori Evaluation: Clustering Error

To evaluate the clustering of TDs, three different errors are used. They all compare characteristics of synthetic time series ( $\tilde{ts}$ ) built from the TDs to the original one ( $ts$ ). The different attributes ( $a \in A$ ) considered are the ones presented in Figure 1a. The same weights ( $\omega_a$ ) as in Equation (1) are used.

The time series error (TSE) (Equation (2)) evaluates if the value is accurate for each hour of the year and each time series:

$$TSE = \sum_{a \in A} \omega_a \sum_{t=1}^{8760} |ts(a, t) - \tilde{ts}(a, t)| \quad (2)$$

The duration curve error (DCE) (Equation (3)) compares the duration curve of the original time series ( $dc$ ) and synthetic time series ( $\tilde{dc}$ ) to quantify the error in the statistical distribution:

$$DCE = \sum_{a \in A} \omega_a \sum_{t=1}^{8760} |dc(a, t) - \tilde{dc}(a, t)| \quad (3)$$

The correlation error (CE) between attributes across all regions (Equation (4)) compares the correlation between each pair of original time series ( $corr(ts(a_1, t), ts(a_2, t))$ ) and the corresponding pair of synthetic time series ( $corr(\tilde{ts}(a_1, t), \tilde{ts}(a_2, t))$ ):

$$CE = \sum_{a_1 \in A} \sum_{a_2 \in A} \omega_{a_1} \omega_{a_2} |corr(ts(a_1, t), ts(a_2, t)) - corr(\tilde{ts}(a_1, t), \tilde{ts}(a_2, t))| \quad (4)$$

#### 2.3.2. A Posteriori Evaluation: Design Error

The error in the whole-energy system design is not trivial to define. Firstly, because it has a high number of elements: 120 technologies and 19 resources per region. All these elements differ in nature and cannot be compared directly. Secondly, because it is complex to differentiate the error due to lower temporal resolution from another phenomenon inducing changes in the results. The typology of the problem studied has a flat optimum. It implies that several solutions are as good as the optimal one. They could be the solution to the reference case with nearly no change in cost. In our case, with a decreased temporal resolution, other changes occur due to reduced accuracy. This is the error we want to quantify. For specific cases and elements, it is possible to underline the causes of the changes, but it is too complex to generalise it to the entire energy system, even more within

a sector- and region-coupled energy system. This issue is further presented and explained in Appendix A.

To study the sensitivity of this kind of model, it is then relevant to explore and summarize its main results: (i) the annualised total cost of the system (objective function), (ii) the size and cost of energy conversion assets, (iii) the quantity and cost of primary energy resources and (iv) the size of interconnections and quantity of energy exchanged. Analysing the objective function is not sufficient to detect the impact of TDs on the energy system results. The size of interconnections and quantity of energy exchanged depends directly on the installed technologies and primary energy used in each region. Therefore, we define the size of each conversion technology and the use of each primary energy, in each region, as an element of interest. From there, we develop a bottom-up approach to quantify the upper bound of the error on all the elements:

1. Compared to the reference case, a threshold of 5% error on an element is arbitrarily defined as acceptable. In Appendix B, this computation is also made for 2.5% and 7.5% error thresholds on each element to show that the results are not very sensitive to this value;
2. At each number of TDs ( $N_{td}$ ), the elements with an error above this threshold are considered as not well represented (set  $W$ ). The apparent design error ( $aDE$ ) is defined as the share of the total cost these elements represent:

$$aDE(N_{td}, ref) = \frac{\sum_{tech \in W} [C_{inv_{ann}}(tech) + C_{maint}(tech)] + \sum_{pe \in W} C_{op}(pe)}{TotalCost} \quad (5)$$

with  $C_{inv_{ann}}(tech)$  being the annualised investment cost of a technology,  $C_{maint}(tech)$  being the maintenance cost of a technology,  $C_{op}(pe)$  being the annual operational cost of a primary energy and  $TotalCost$  being the annualised total cost of the system;

3. Because of the flat optimum and the oscillating behaviour, this apparent design error is the superposition of the design error ( $DE(N_{td}, ref)$ ) we want to compute and a random noise ( $\delta(N_{td})$ ):

$$aDE(N_{td}, ref) = DE(N_{td}, ref) + \delta(N_{td}) \quad (6)$$

4. To reduce this noise, the design error is computed for each number of TDs as the minimum of the apparent design error for lower or equal number of TDs:

$$DE(N_{td}, ref) = \min_{\forall t \leq N_{td}} aDE(N_{td}, ref) \quad (7)$$

### 3. Case Studies

This section describes the cases studied to test the methodology. First, common assumptions for all cases are presented. Then, the nine cases with different numbers and typologies of regions are presented. All these cases are examples used to develop and validate the method but are not the main focus of this work.

The following assumptions are common to all cases:

- The weather and consumption data of the year 2015 are used to build the time series of the different attributes [63,64];
- The target year 2035 is used to forecast costs, efficiency, end-use demands, etc. This year and the regions used are chosen because of data availability from previous studies [63,64]. The macro-regions are built by merging countries together using the methodology of [63] (e.g., Spain and Portugal are merged to build the Iberian peninsula). This methodology regroups neighbouring countries with similar patterns in terms of demands and resources. From these studies, two main changes have been made. Firstly, the maximum installed capacity for nuclear in France is set to 41.3 GW, taken from [65]. Secondly, the onshore wind potential considered here represents only 50% of the total technical potential that was used in these studies. This choice

was made for two reasons: (i) these regions have a very high technical potential for onshore wind. As it is a very cheap source of renewable energy, it outcompetes other renewable sources of energy. (ii) the technical potentials are very high compared to what is currently installed and might never be reached because of social acceptance;

- Having a good temporal resolution is especially important to integrate a high share of VRES. Therefore, to obtain systems with high penetration of VRES, we set the greenhouse gas emission reduction to 90% compared to 1990;
- All regions can import fossil or renewable fuels from the rest of the world but not electricity.

The case studies are built by associating six macro-regions covering Western Europe (Figure 2). In all cases, these macro-regions are considered as one cell each. In multi-regional cases, they can exchange energy carriers between them. They are defined as follows:

- AtChIt: Austria, Switzerland and Italy;
- DeBeNeLux: Germany, Belgium, Netherlands and Luxembourg;
- Scandinavia: Denmark and Sweden;
- Iberian Peninsula: Spain and Portugal;
- France;
- British Islands: Ireland and the United Kingdom.



**Figure 2.** The six macro-regions considered to build the nine case studies: six with 1 cell, one with 2 cells, one with 3 cells and one with 6 cells.

From these regions, the nine case studies are selected for their diversity. Four main differences are considered (Table 1): (i) the ratio between renewable energy potentials (REPs) and final energy consumption (FEC), providing an informed guess of whether the region will be in deficit or in excess in a fossil-free energy system; (ii) the allowed installation of nuclear power plants; (iii) the share of solar in the REPs; (iv) the share of wind in the REPs. Table 1 gives a classification of the cases for these criteria in five categories, from the worst/lowest (- -) to the best/highest (++). In addition, cases with a different number of interconnected regions are considered: one, two, three and six. Having a multi-regional case complexifies the clustering of TDs and might lead to different results from one- to six-region cases. The code at the beginning of the name of each case gives the number of cells.

**Table 1.** Diversity of considered cases. Four influential characteristics are compared qualitatively and classified into five categories, from the lowest (-) to the highest (++): (i) ratio between renewable energy potentials (REP) and final energy consumption (FEC); (ii) investment in nuclear power plants allowed; (iii) share of solar in REPs; (iv) share of wind in REPs.

Test Case	REP/FEC <sup>1</sup>	Nuclear	Solar	Wind
1R-AtChIt	-	--	+	-
1R-DeBeNeLux	--	--	+ -	+
1R-Scandinavia	++	--	--	++
1R-Ib.Peninsula	++	--	++	+ -
1R-France	+ -	++	+	+ -
1R-Brit.Islands	+ -	--	+ -	++
2R-DBNL-Fr	-	+	+	+ -
3R-AtlanticEU	+	+	+	+
6R-WesternEU <sup>2</sup>	+ -	+ -	+	+

<sup>1</sup> For all case studies, the renewable energy potentials are derived from [66,67], and the final energy consumption from [68]. In this column, the symbols indicate ranges of the ratio REP/FEC: (-)  $REP/FEC < 1$ , (-)  $REP/FEC \in [1; 1.25[$ , (+ -)  $REP/FEC \in [1.25; 1.75[$ , (+)  $REP/FEC \in [1.75; 2[$ , (+ +)  $REP/FEC \geq 2$ . The range at the margin to supply its demand with RES has been chosen to be around 1.5 to account for losses from primary energy to final energy. <sup>2</sup> For the case with 6 regions, we could not solve the full-year case on our machine due to a lack of memory. The following conservative approach has been used to fill this lack of data: the case with the highest number of TDs (i.e., 180) has been taken as the reference, and the design errors computed have been shifted up by the error at 180 TDs taken from the 3-region case.

From Table 1, the cases' characteristics can be summarized as follows:

- 1R-AtChIt: one-region case with a small deficit of renewable energy source potentials, mostly oriented towards photovoltaic panels;
- 1R-DeBeNeLux: one-region case with a high deficit of renewable energy source potentials, a substantial potential for wind turbines and lower photovoltaic;
- 1R-Scandinavia: one-region case with a high excess of renewable energy source potentials, especially in terms of wind power;
- 1R-Ib.Peninsula: one-region case with a high excess of renewable energy source potentials, especially in terms of photovoltaics;
- 1R-France: one-region case at the margin in terms of renewable energy source potentials but allowed to invest in nuclear power;
- 1R-Brit.Islands: one-region case at the margin in terms of renewable energy source potentials, without nuclear and with its main potential being wind;
- 2R-DBNL-Fr: two-region case (i.e., DeBeNeLux interconnected with France) with a small deficit of renewable energy sources but with nuclear power allowed in France;
- 3R-AtlanticEU: three-region case (i.e., Iberian Peninsula, France and British Islands interconnected) with a small excess of renewable energy source potentials, some nuclear in France and good photovoltaic and wind potentials;
- 6R-WesternEU: six-region case at the margin in terms of renewable energy source potentials, some nuclear in France and good photovoltaic and wind potentials.

#### 4. Results and Discussion

This section presents and discusses the error evaluations for all cases. First, it illustrates the gain in computational tractability with the number of TDs. Then, it evaluates the *a priori* errors. Afterwards, the sensitivity of the energy system results is studied. Finally, the *a priori* and *a posteriori* metrics are compared, and a method for any new case study is proposed. In all figures, the one-region cases have the same colours as in Figure 2, and the multi-region cases have different shades of grey.

#### 4.1. Gain in Computational Tractability

Figure 3 provides the gain in computational time of each model evaluation compared to the full-year resolution. The optimisation problem is solved using the commercial software IBM CPLEX 12.9 with a barrier algorithm on an Intel®Core™ Quad i9-10980XE CPU @3.0 GHz, with a memory of 128 GB. The oscillation is due to the fact that the optimisation problem changes slightly by changing the number of TDs. Hence, the polyhedron of the feasible solutions changes, and the algorithm might not always converge faster when slightly decreasing the number of TDs. The optimisation was run several times in the case of the biggest oscillation to make sure it did not come from other causes. However, when solving many numbers of TDs, a general trend can be seen. The gain in solving time is mostly significant below 90 TDs, in particular for multi-regional cases. Hence, our range of interest is 2 to 90 TDs. The different errors are studied in this range.

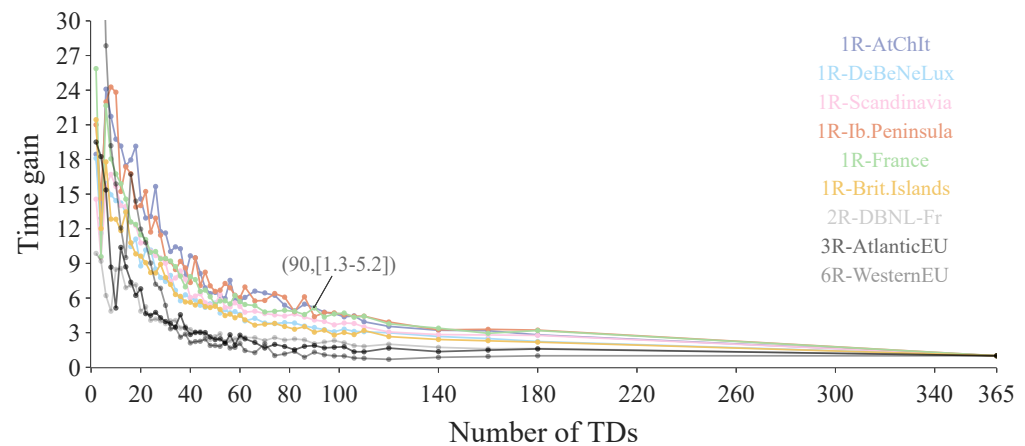


**Figure 3.** Time gain expressed as the ratio of the computational time with full-year resolution to the one with lower numbers of typical days (TDs) for all case studies.

#### 4.2. A Priori Evaluation: Clustering Error

Figures 4–6 present the evolution of the time series error (*TSE*), the duration curve error (*DCE*) and the correlation error (*CE*). They evaluate, respectively, whether the time series at each hour of the year, their distribution and the relationship between time series are well represented. These errors are studied as they are the most common in the literature, and they are easy to evaluate *a priori*. It makes them convenient to choose the number of TDs at a low cost for a new case study.

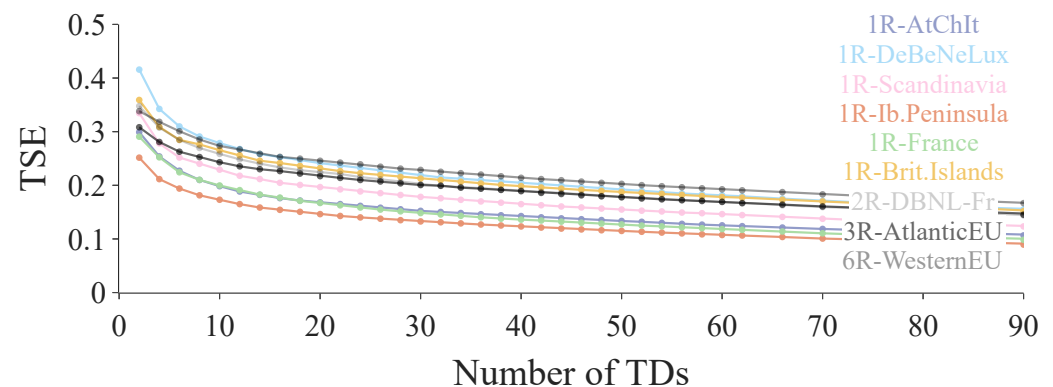


**Figure 4.** Evolution of the time series error (*TSE*) with the number of typical days (TDs) for all case studies.

For all cases, up to 20 TDs, these errors decrease rapidly. At a higher number of TDs, the time series error decreases linearly, whereas the other errors stay very low and are

nearly constant. Hence, the time series error is the only *a priori* error that keeps a certain sensitivity to the number of TDs above 20 TDs. At this stage, it is not possible to formally define the acceptable threshold for these errors.

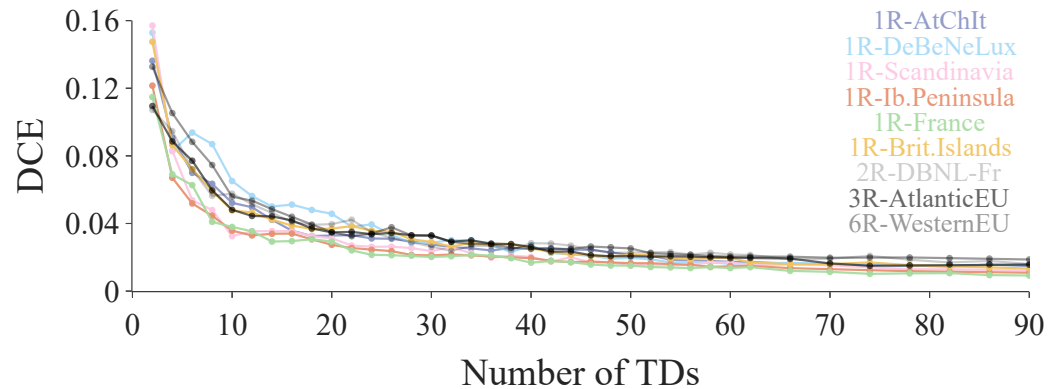


**Figure 5.** Evolution of the duration curve error (*DCE*) with the number of typical days (TDs) for all case studies.

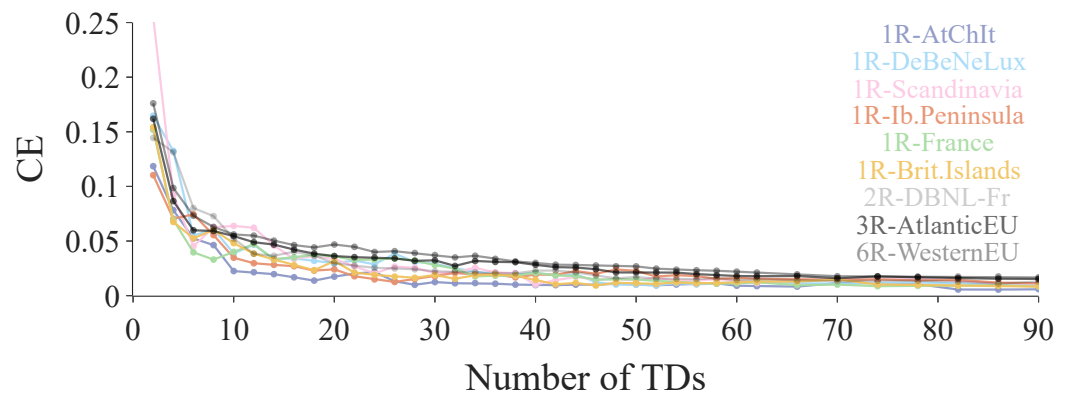


**Figure 6.** Evolution of the correlation error (*CE*) with the number of typical days (TDs) for all case studies.

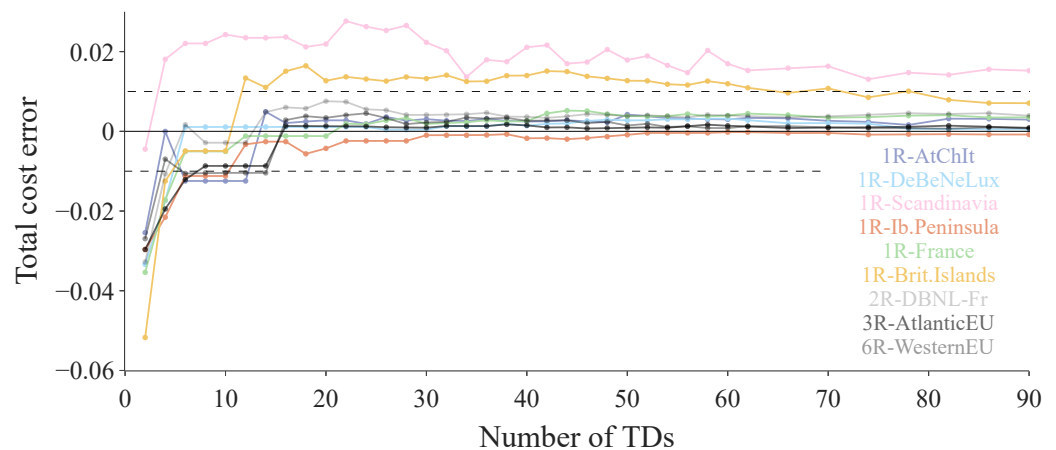
#### 4.3. A Posteriori Evaluation: Sensitivity of Energy System Results

This subsection studies the sensitivity of the ESOM results to the number of TDs. First, the error on the objective function, i.e., the annualised total cost, is presented. Then, the design error is analysed.

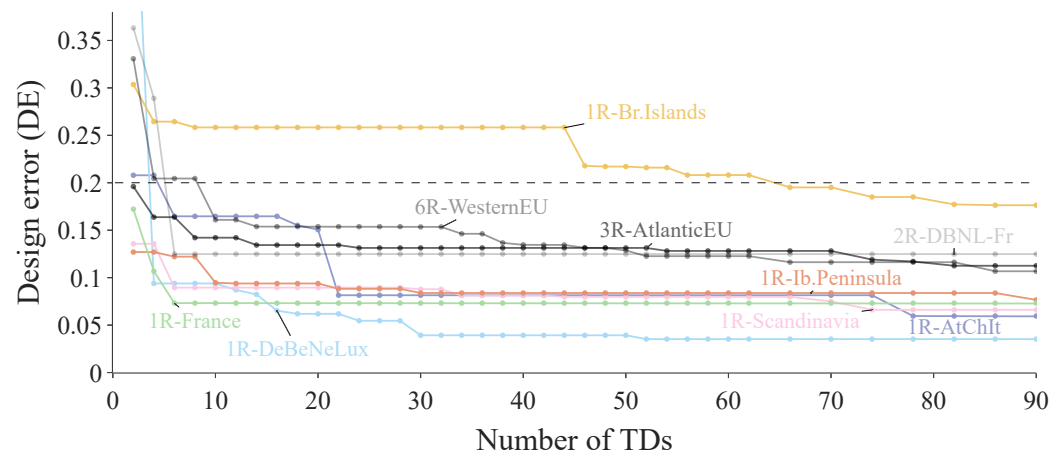
Figure 7 presents the relative error on the total annualised cost of the system as a function of the number of TDs. The error decreases rapidly at low numbers of TDs for all cases and then stagnates over the entire range. Above 14 TDs, the error is below 1% for all cases except for 1R-Scandinavia and 1R-Brit.Islands. In these two cases, the total cost is overestimated. In general, the error on the total cost stays very low for any number of TDs. It is thus not the best metric to evaluate the error in the energy system results. Indeed, very expensive technologies (e.g., private cars) are quite insensitive to the temporal resolution. On the contrary, some key technologies for the security of supply (e.g., seasonal thermal storage) might represent a lower share of the total cost and be very sensitive to the number of TDs. A closer look at the error in the investments in the assets and the primary resources used over the year is necessary.

Figure 8 depicts the design error for all cases. In all cases, except 1R-Brit.Islands, at 10 TDs, most of the gain in accuracy is achieved, and an error below 20% is reached (i.e.,  $DE \in [7.3; 16.1]\%$ ). Using 10 TDs divides the computational time by 8.6 to 23.8, according to the case. The 1R-Brit.Islands case needs 46 TDs to have a significant gain in accuracy and 66 TDs to reach an error below 20%. However, as described in Table 1, this case has particular characteristics that can be detected *a priori*. Indeed, it is the only case with just enough

renewable energy potentials to supply its final energy consumption (i.e.,  $REP/FEC = 1.47$  or “(+ −)” in Table 1), and no possibility to install a low-carbon nuclear baseload. Thus, it is more sensitive to the quality of the temporal representation. Indeed, a bad temporal representation leads to an underestimation of the intermittency of renewables. Hence, it overestimates their contribution and needs to import fewer fuels from outside of the system to compensate for their intermittency with dispatchable energy sources. For the other one-region cases, the design error can be further reduced by increasing from 10 to 24 TDs, if needed. On the contrary, for the multi-regional cases, only a small reduction in the design error can be achieved above 10 TDs (i.e., at the most, 4.7% by using 90 TDs).



**Figure 7.** Evolution of the error on the annualised total cost (objective function) with the number of typical days (TDs) for all cases. The dashed line represents the threshold of the error at 1%.



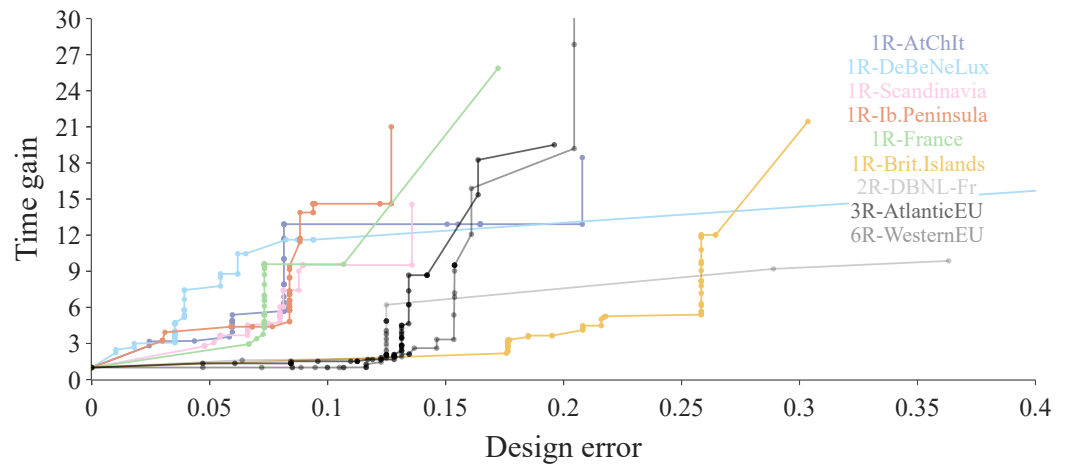
**Figure 8.** Evolution of the design error (DE) with the number of typical days (TDs) for all case studies.

Figure 9 underlines the trade-off between time gain and design error. It is a combination of Figures 3 and 8. The more a point is in the upper-left corner of the graph (i.e., high time gain and low design error), the better the trade-off is. Hence, the best trade-offs are at the top of the long vertical section of each curve.

Here, again, the case 1R-Brit.Island stands out, as it always displays a high design error. To reach a design error below 20%, its time gain falls down to 3.7. Another choice could be to favor time gain (up to 12) at the cost of a higher design error (25.8%). Otherwise, other temporal aggregation techniques could be tested and perform better on this type of case (e.g., adding manually extreme days after the TD clustering). This could be explored in future works using the developed design error.

The other cases can be divided into two categories on this graph: (i) the one-region cases have good trade-offs with a time gain of 9.5 to 14.6 and a design error below 10%;

(ii) the multi-regional case also reach high time gain at the best trade-off (6.2 to 16.1) but have a higher design error (between 12 and 16%). For all these cases, the best trade-offs correspond to the points at 10 TDs already analysed on the basis of Figure 8.



**Figure 9.** Relation between time gain and design error. The more a point is in the upper-left corner the better it is (i.e., high time gain and low design error). For each curve, the best trade-off lies at the top of the vertical section.

#### 4.4. Comparison of a Priori and a Posteriori Errors

This subsection studies the correlation between *a priori* and *a posteriori* metrics. *A priori* errors can be evaluated without solving the ESOM. Hence, they could allow to select the number of TDs at a low computational cost. Indeed, the clustering of TDs has a low computational cost (i.e., around 10 to 20 s), and it only needs to be computed once for many scenarios in the same geographical area.

Table 2 reports the significant correlation between the design error and the different *a priori* errors. In particular, the time series error has a correlation above 0.9 in most cases. Hence, it is investigated in further detail.

**Table 2.** Correlation between *a priori* and *a posteriori* errors for all cases.

Test Case	Time Series Error	Duration Curve Error	Correlation Error
1R-AtChIt	0.92	0.85	0.75
1R-DeBeNeLux	0.68	0.83	0.83
1R-Scandinavia	0.94	0.76	0.66
1R-Ib.Peninsula	0.90	0.68	0.70
1R-France	0.69	0.76	0.79
1R-Brit.Islands	0.90	0.64	0.54
2R-DBNL-Fr	0.71	0.77	0.82
3R-AtlanticEU	0.93	0.73	0.69
6R-WesternEU	0.91	0.92	0.94

Figure 10 gives more insights into these correlations. It presents the design error and the time series error for all cases and for all points evaluated. If we discard the particular case of 1R-Brit.Islands, most of the points (99.5%) are concentrated below the curve  $DE = TSE$ . Hence, the time series error can be considered a good prediction of the upper bound of the design error. In addition, the points can be approximated by the linear relationship  $DE = 0.75 TSE$ . This relation is still conservative as most of the points (85.7%) lie below this curve.

As discussed previously, the 1R-Brit.Islands case behaves differently than the others. However, this can be detected *a priori* by computing the ratio  $REP/FEC$ , and the rule

to select the number of TDs based on the time series error can be adapted to a more conservative approach. The points of this case stay close to the curve  $DE = TSE$ , and for the trade-off at 46 TDs found in Figure 8,  $DE = TSE + 0.03$ .

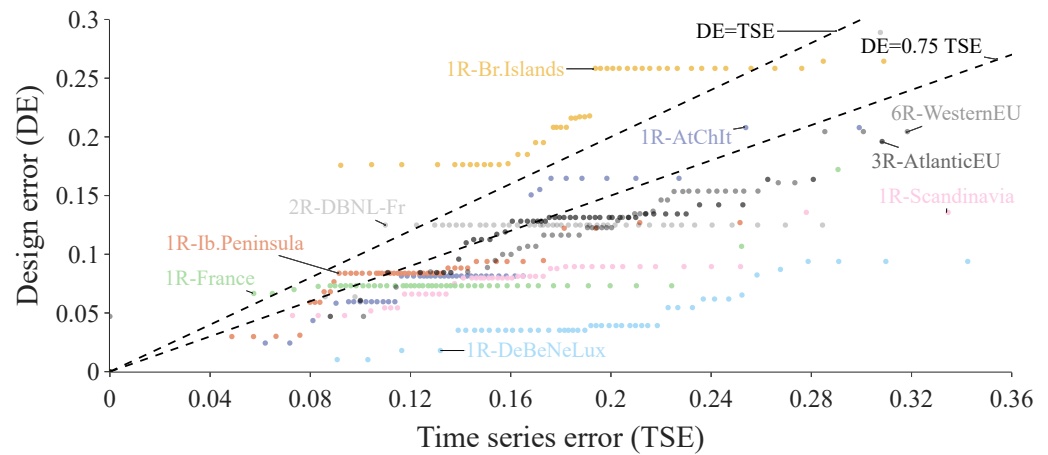


**Figure 10.** Design error (DE) vs. time series error (TSE) for all cases and all numbers of TDs evaluated (i.e., 432 model evaluations). The 1-region cases are depicted in colours, and the multi-region cases are in shades of grey. A line for  $DE = TSE$  and a line for  $DE = 0.75 TSE$  are represented to underline that, discarding the particular case 1R-Brit.Islands, (i) all points are located below the first line; (ii) the second line is a good linear approximation of the relation between DE and TSE.

To conclude, the time series error provides a good estimation of the design error that can be expected. Hence, it can be used to select the number of TDs for a new case study. Two different cases have to be considered according to the ratio between renewable energy potentials (REP) and final energy consumption (FEC):

1. In most cases, the time series error can be used to select the number of typical days with the relation:

$$DE = 0.75 TSE \quad (8)$$

From the cases studied, a value of  $DE = 0.165$  or  $TSE = DE/0.75 = 0.22$  gives a good trade-off between accuracy and computational tractability;

2. In the particular cases where  $REP/FEC \in [1.25; 1.75[$  and no other low-carbon baseload production is available (e.g., nuclear power), the energy system results are more sensitive to the temporal resolution. The relation above does not work, but the design error and time series error stay close in value. Hence, we can use the following relation:

$$DE = TSE \quad (9)$$

For instance, in the case studied that falls into this category (i.e., 1R-Brit.Islands), the best trade-off between accuracy and computational tractability is at  $DE = 0.22$  and  $TSE = 0.19$ .

## 5. Conclusions and Perspectives

Methods to speed up energy system optimisation models (ESOMs) while keeping good accuracy are essential to consider the uncertainty inherent to long-term planning. Typical day (TD) clustering is a well-established method that can significantly improve the computational tractability. The clustering error (*a priori*) has been thoroughly studied in the literature, but its impact on the accuracy of the energy system optimisation results (*a posteriori*) is rarely studied in depth. This paper analyses this impact by applying, for different numbers of TDs, the multi-regional whole-energy system model, EnergyScope Multi-Cells, to nine cases with different typologies and number of regions. A bottom-up

design error is developed to evaluate the impact on the results by (i) selecting the elements (i.e., technologies sizes or primary energy uses) with an unacceptable error (i.e., above 5%) and (ii) defining the design error as the share of the total annualised cost that these elements represent. Then, this design error is compared with the commonly used *a priori* errors (i.e., time series, duration curve and correlation errors).

In all cases, we underline a strong correlation between the design error and the time series error. This *a priori* metric gives a good estimation of the upper bound on the design error and can be used to choose the number of TDs in any new case study without having to evaluate the ESOM. However, our analysis reveals that cases can fall into two categories to define the exact relationship between design error and time series error. The first category gathers most of the cases. Here, a trade-off is found at 10 TDs, which is ensured to have a design error lower than 17% and runs 8.6 to 23.8 times faster than the full-year model evaluation according to the case. In those cases, the design error is lower than the time series error in 99.5% of the model evaluations performed, and it can be approximated by the linear relation  $DE = 0.75 TSE$ . As an indicative value, the results of this study suggest taking  $DE = 0.165$  or  $TSE = 0.22$ . The second category is a particular case that can be detected *a priori* by looking at the ratio between the renewable energy potentials (REPs) and the final energy consumption (FEC), and the possibility of installing low-carbon baseload (e.g. nuclear power). This particular case corresponds to  $REP/FEC \in [1.25; 1.75[$  and no low-carbon baseload allowed. It is more sensitive to the temporal resolution than the other cases. For this type of case, this study suggests using a more conservative relation between design error and time series error:  $DE = TSE$ . In addition, this category does not reach as low a design error as the other, even when increasing the number of TDs. From our results, we advise aiming for  $DE = TSE = 0.19$  for this type of case. In our study, this is equivalent to taking 46 TDs which implies a model evaluation that runs 5.7 times faster than the full year. All those observations work both for 1-region and multi-regional cases. It proves that the TD approach can be extended to multi-regional whole-energy systems.

To increase the confidence in these conclusions, they should be tested with other models and in other case studies, with another reference year for the time series, other technologies, etc. In addition, other limitations of this study could lead to future works: (i) To evaluate the accuracy of optimisation results with a lower temporal resolution, they are compared to the full-year model evaluation. It implies that it should be feasible to run this full-year model. Furthermore, due to the flat optimum of the optimisation problem, the design error has an oscillating behaviour that makes it hard to interpret. Another approach to assess the quality of the solutions obtained would be to run a more accurate operation model and evaluate its adequacy. (ii) The clustering algorithm and its hyper-parameter were chosen based on the literature. With the newly developed method, it could be fine-tuned and compared to other algorithms. In particular, the ability of the clustering algorithm to include the extreme events was not assessed specifically in this work. (iii) TD clustering is only one of the performance enhancement techniques. A trade-off between the number of TDs and other techniques, such as spatial aggregation, could exist. Here also, the developed method to evaluate the loss of accuracy in optimisation results could be used to find such a trade-off.

To conclude, this study focuses on developing a relevant *a posteriori* metric (i.e., the design error) to evaluate the impact of TDs clustering on ESOMs results. It compares it with the widely used *a priori* metrics (i.e., time series, duration curve and correlation errors). This comparison reveals that the time series error is a conservative estimation of the design error. Hence, it can be used to select *a priori* the number of TDs to reach a certain accuracy on the ESOM results. In addition, this work paves the way for many other works on performance enhancement techniques. Indeed, with a powerful metric that is easily applicable to any ESOM and any case study, it is possible to compare and assess the best performance enhancement techniques for a specific case.

**Supplementary Materials:** The following supporting information can be consulted online at <https://energyscope-multi-cells.readthedocs.io/en/master/> (accessed on 1 January 2023). It describes EnergyScope Multi-Cells, the multi-regional whole-energy system optimisation model used for this study.

**Author Contributions:** The model development, the case study, the data analysis and the paper writing were performed by P.T. The supervision, funding and review of the work were performed by H.J. and F.C. All authors have read and agreed to the published version of the manuscript.

**Funding:** The authors acknowledge the support of the Energy Transition Fund of Belgium.

**Data Availability Statement:** The data presented in this study are openly available on Zenodo at <https://doi.org/10.5281/zenodo.7527344> (accessed on 1 February 2023). The input data, the actual version of the model, the output data and analysis script can be found there. The model used is still under construction; the up to date version can be found at [https://github.com/energyscope/EnergyScope\\_multi\\_cells](https://github.com/energyscope/EnergyScope_multi_cells) (accessed on 27 January 2023).

**Conflicts of Interest:** The authors declare no conflict of interest. The funders had no role in the design of this study; in the collection, analyses, or interpretation of data; in the writing of the manuscript; or in the decision to publish the results.

## Abbreviations

The following abbreviations are used in this manuscript:

1R	1 region
2R	2 interconnected regions
3R	3 interconnected regions
6R	6 interconnected regions
<i>aDE</i>	apparent design error
AtChIt	Austria, Italy and Switzerland
AtlanticEU	Interconnected Atlantic European Countries (i.e., British Islands, France and Iberian Peninsula)
Brit.Islands	British Islands (i.e., Ireland and United Kingdom)
<i>CE</i>	Correlation error
DBNL-Fr	DeBeNeLux interconnected with France
<i>DCE</i>	Duration curve error
<i>DE</i>	Design error
DeBeNeLux	Germany, Belgium, Netherlands and Luxembourg
ES-PT	Spain and Portugal (or Iberian peninsula)
ESOM	Energy system optimisation model
FEC	Final energy consumption
FR	France
GHz	Gigahertz
GW	Gigawatts
HVC	High value chemicals
Ib.Peninsula	Iberian Peninsula (i.e., Spain and Portugal)
IE-UK	Ireland and United Kingdom (or British Islands)
PV	Photovoltaic panels
REP	Renewable energy potential
RES	Renewable energy sources
TD	Typical day
<i>TSE</i>	Time series error
VRES	Variable renewable energy sources
WesternEU	Interconnected Western European Countries (i.e., Alp.States, DeBeNeLux, Scandinavia, France and Brit.Islands)

## Appendix A. Oscillation in Design Error and Smoothing

This section explains in more detail the oscillating behaviour of the design error. The 3R-AntlanticEU case is used as an example to present this phenomenon, but it could

be underlined in any case study. Firstly, the difference between apparent design error (aDE) and design error is illustrated. Then, an example of changes due to the flat optimum is presented.

As explained in Section 2.3.2, the optimisation of the design and operation of large integrated energy systems has a flat optimum. Indeed, several equivalent solutions exist with different designs. This explains the interest in near-optimal solutions exploration in the field [69–75]. Figure A1 presents the difference between the apparent design error and the design error. There is an oscillating behaviour where sometimes a higher number of typical days (TDs) leads to a higher design error. The problem considered is a whole-energy system where the different energy sectors are highly coupled. It leads to complex energy systems where all decisions are linked. Hence, it is not possible to determine, in general, which part of the error comes from the lower temporal resolution and which part comes from the flat optimum. However, when an increase in the number of TDs implies an increase in design error, this is most likely due to a switch from an equivalent solution to another. Therefore, we can approximate the design error at a certain number of TDs by the minimum of the apparent design error for this number or lower numbers of TDs (Equation (7)). This reveals a part of the oscillation due to the flat optimum, but there is no way to prove that it considers its whole effect.

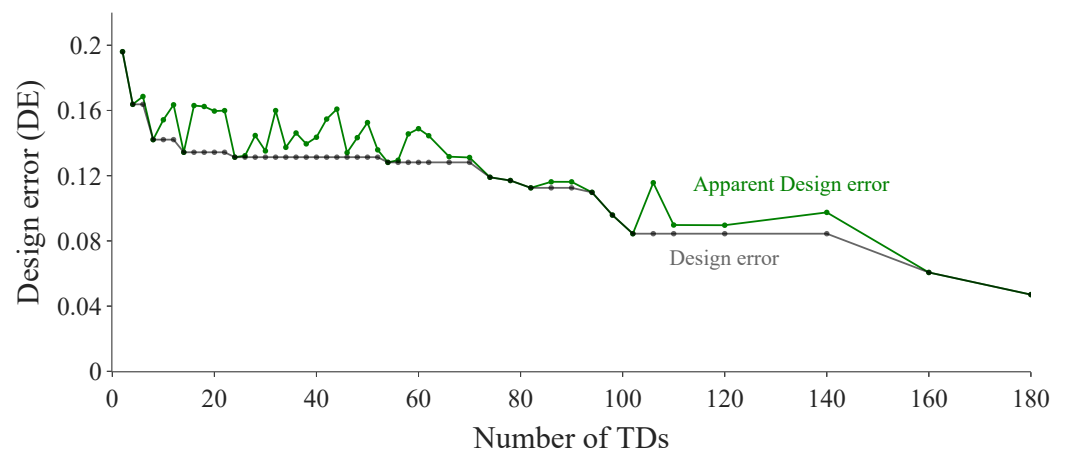


**Figure A1.** Evolution of the apparent design error and the design error for the 3R-AtlanticEU case study. The apparent design error has an oscillating behaviour due to the flat optimum of the optimisation problem. Therefore, it is approximated by its lower bound.

Figure A2 provides an example of oscillating behaviour due to the flat optimum. It presents the relative error in assets and resources used to provide the non-energy demand for high-value chemicals (HVC) for the British Islands in the 3R-AtlanticEU case study. There are two competing routes: (i) importing more renewable methanol and converting it to HVC (i.e., green and orange curves); (ii) importing more oil, converting it to HVC, and emitting less in other energy sectors (i.e., blue curve). The error on those two options oscillates in opposite directions from one number of TDs to the other. This even occurs at a high number of TDs, with very accurate temporal resolution. For instance, the relative error on those elements becomes very small at 102 and 120 TDs and increases both between and after those numbers. This shows that those two options are equivalent.

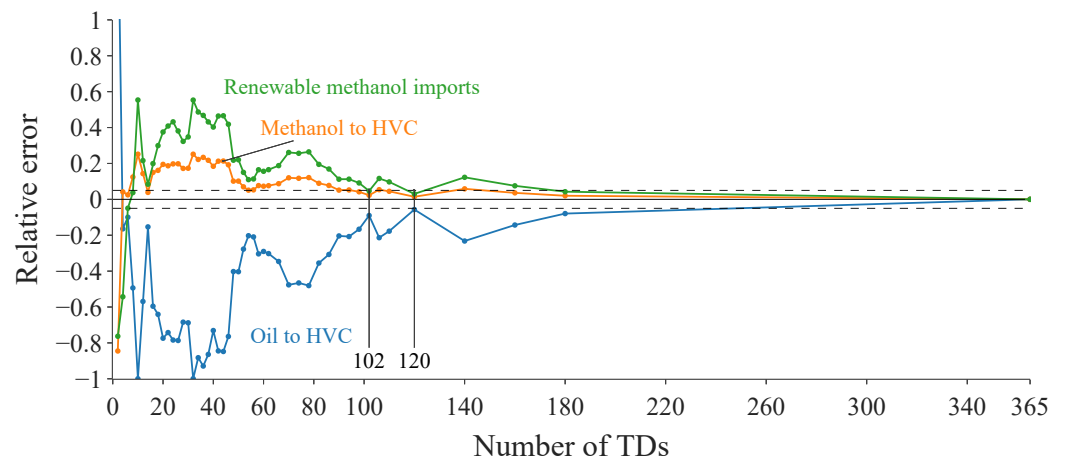


**Figure A2.** Example of oscillating elements in the production of high-value chemicals (HVC) for the British Islands for the case 3R-AtlanticEU. At high numbers of TDs, the problem oscillates between two equivalent solutions: one with more production from renewable methanol and less from oil and another with the opposite.

### Appendix B. Impact of the Threshold on the Elements Error

Based on the approach explained in Section 2.3.2, Figure A3 is built, taking different acceptable thresholds for the error on elements (2.5, 5 and 7.5%). This is performed on the 3R-AtlanticEU case study to illustrate the results, but it could be extended to any other case. Taking those acceptable threshold increases or decreases, respectively, the design error by less than 3.5%. In addition, the general shape of the curve stays unchanged; that is, most of the gain in accuracy is reached around 14 TDs, and then the error is nearly constant. As the goal of this metric is to find trade-offs between the accuracy of the model results and computational cost, any of those thresholds are equivalent.

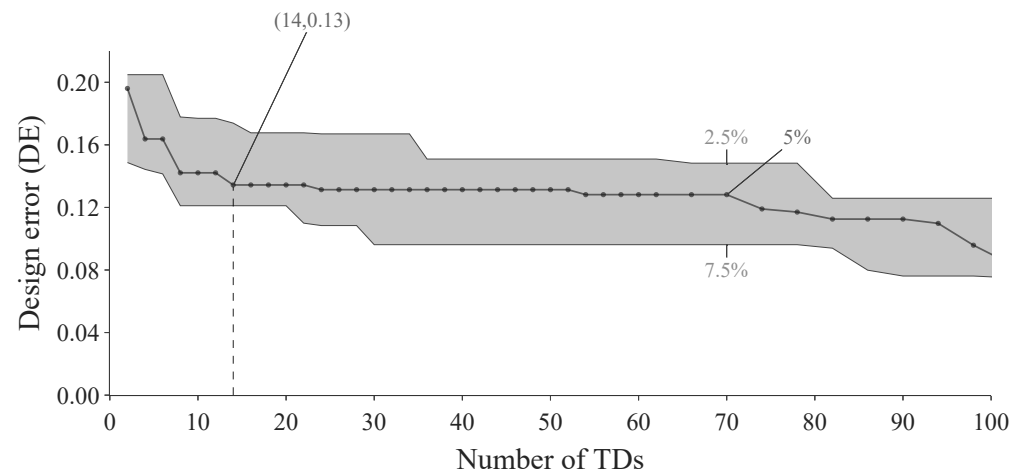


**Figure A3.** Evolution of the design error (DE) with the number of typical days (TDs) for the 3R-AtlanticEU case study. The grey curve is made with the reference threshold of 5% for the error on each element. The grey area around it is obtained by exploring the sensitivity of this threshold down to 2.5% and up to 7.5%.

### References

1. Pfenninger, S.; Hawkes, A.; Keirstead, J. Energy systems modeling for twenty-first century energy challenges. *Renew. Sustain. Energy Rev.* **2014**, *33*, 74–86. [\[CrossRef\]](#)
2. Contino, F.; Moret, S.; Limpens, G.; Jeanmart, H. Whole-energy system models: The advisors for the energy transition. *Prog. Energy Combust. Sci.* **2020**, *81*, 100872. [\[CrossRef\]](#)

3. Chang, M.; Thellufsen, J.Z.; Zakeri, B.; Pickering, B.; Pfenninger, S.; Lund, H.; Østergaard, P.A. Trends in tools and approaches for modelling the energy transition. *Appl. Energy* **2021**, *290*, 116731. [[CrossRef](#)]
4. Moret, S.; Gironès, V.C.; Bierlaire, M.; Maréchal, F. Characterization of input uncertainties in strategic energy planning models. *Appl. Energy* **2017**, *202*, 597–617. [[CrossRef](#)]
5. Rixhon, X.; Limpens, G.; Coppitters, D.; Jeanmart, H.; Contino, F. The role of electrofuels under uncertainties for the Belgian energy transition. *Energies* **2021**, *14*, 4027. [[CrossRef](#)]
6. Cao, K.K.; Krbek, K.V.; Wetzel, M.; Cebulla, F.; Schreck, S. Classification and evaluation of concepts for improving the performance of applied energy system optimization models. *Energies* **2019**, *12*, 4656. [[CrossRef](#)]
7. Prina, M.G.; Manzolini, G.; Moser, D.; Nastasi, B.; Sparber, W. Classification and challenges of bottom-up energy system models—A review. *Renew. Sustain. Energy Rev.* **2020**, *129*, 109917. [[CrossRef](#)]
8. Flores-Quiroz, A.; Palma-Behnke, R.; Zakeri, G.; Moreno, R. A column generation approach for solving generation expansion planning problems with high renewable energy penetration. *Electr. Power Syst. Res.* **2016**, *136*, 232–241. [[CrossRef](#)]
9. Roh, J.H.; Shahidehpour, M.; Fu, Y. Market-based coordination of transmission and generation capacity planning. *IEEE Trans. Power Syst.* **2007**, *22*, 1406–1419. [[CrossRef](#)]
10. Binato, S.; Pereira, M.V.F.; Granville, S. A new Benders decomposition approach to solve power transmission network design problems. *IEEE Trans. Power Syst.* **2001**, *16*, 235–240. [[CrossRef](#)]
11. Haikarainen, C.; Pettersson, F.; Saxén, H. A decomposition procedure for solving two-dimensional distributed energy system design problems. *Appl. Therm. Eng.* **2016**, *100*, 30–38. [[CrossRef](#)]
12. Romero, R.; Monticelli, A. A hierarchical decomposition approach for transmission network expansion planning. *IEEE Trans. Power Syst.* **1994**, *9*, 373–380. [[CrossRef](#)]
13. Poncelet, K.; Delarue, E.; Six, D.; Duerinck, J.; D'haeseleer, W. Impact of the level of temporal and operational detail in energy-system planning models. *Appl. Energy* **2016**, *162*, 631–643. [[CrossRef](#)]
14. Kotzur, L.; Nolting, L.; Hoffmann, M.; Groß, T.; Smolenko, A.; Priesmann, J.; Büsing, H.; Beer, R.; Kullmann, F.; Singh, B.; et al. A modeler's guide to handle complexity in energy systems optimization. *Adv. Appl. Energy* **2021**, *4*, 100063. [[CrossRef](#)]
15. Frew, B.A.; Jacobson, M.Z. Temporal and spatial tradeoffs in power system modeling with assumptions about storage: An application of the POWER model. *Energy* **2016**, *117*, 198–213. [[CrossRef](#)]
16. Hoffmann, M.; Kotzur, L.; Stolten, D.; Robinius, M. A review on time series aggregation methods for energy system models. *Energies* **2020**, *13*, 641. [[CrossRef](#)]
17. Hoffmann, M.; Priesmann, J.; Nolting, L.; Praktiknjo, A.; Kotzur, L. Typical periods or typical time steps? A multi-model analysis to determine the optimal temporal aggregation for energy system models. *Appl. Energy* **2021**, *304*, 117825. [[CrossRef](#)]
18. Hoffmann, M.; Kotzur, L.; Stolten, D. The Pareto-Optimal Temporal Aggregation of Energy System Models. *Appl. Energy* **2022**, *315*, 119029. [[CrossRef](#)]
19. Teichgraber, H.; Brandt, A.R. Time-series aggregation for the optimization of energy systems: Goals, challenges, approaches, and opportunities. *Renew. Sustain. Energy Rev.* **2022**, *157*, 111984. [[CrossRef](#)]
20. Anderski, T.; Surmann, Y.; Stemmer, S.; Grisey, N.; Momot, E.; Leger, A.C.; Betraoui, B.; Van Roy, P. *European Cluster Model of the Pan-European Transmission Grid*; Technical Report, eHIGHWAY2050; European Network of Transmission System Operators for Electricity: Brussels, Belgium, 2014.
21. Horsch, J.; Brown, T. The role of spatial scale in joint optimisations of generation and transmission for European highly renewable scenarios. In Proceedings of the 14th International Conference on the European Energy Market (EEM), Dresden, Germany, 6–9 June 2017; pp. 1–7. [[CrossRef](#)]
22. Schaber, K.; Steinke, F.; Hamacher, T. Transmission grid extensions for the integration of variable renewable energies in Europe: Who benefits where? *Energy Policy* **2012**, *43*, 123–135. [[CrossRef](#)]
23. Aryanpur, V.; O'Gallachoir, B.; Dai, H.; Chen, W.; Glynn, J. A review of spatial resolution and regionalisation in national-scale energy systems optimisation models. *Energy Strateg. Rev.* **2021**, *37*, 100702. [[CrossRef](#)]
24. Martínez-Gordón, R.; Morales-España, G.; Sijm, J.; Faaij, A.P. A review of the role of spatial resolution in energy systems modelling: Lessons learned and applicability to the North Sea region. *Renew. Sustain. Energy Rev.* **2021**, *141*, 110857. [[CrossRef](#)]
25. Tröndle, T.; Lilliestam, J.; Marelli, S.; Pfenninger, S. Trade-Offs between Geographic Scale, Cost, and Infrastructure Requirements for Fully Renewable Electricity in Europe. *Joule* **2020**, *4*, 1929–1948. [[CrossRef](#)]
26. Munoz, F.D.; Sauma, E.E.; Hobbs, B.F. Approximations in power transmission planning: Implications for the cost and performance of renewable portfolio standards. *J. Regul. Econ.* **2013**, *43*, 305–338. [[CrossRef](#)]
27. Langrené, N.; Ackooij, W.V.; Bréant, F. Dynamic constraints for aggregated units: Formulation and application. *IEEE Trans. Power Syst.* **2011**, *26*, 1349–1356. [[CrossRef](#)]
28. Nolden, C.; Schönfelder, M.; Eßer-Frey, A.; Bertsch, V.; Fichtner, W. Network constraints in techno-economic energy system models: Towards more accurate modeling of power flows in long-term energy system models. *Energy Syst.* **2013**, *4*, 267–287. [[CrossRef](#)]
29. Pfenninger, S. Dealing with multiple decades of hourly wind and PV time series in energy models: A comparison of methods to reduce time resolution and the planning implications of inter-annual variability. *Appl. Energy* **2017**, *197*, 1–13. [[CrossRef](#)]

30. Poncelet, K.; Höschle, H.; Delarue, E.; Virag, A.; D'haeseleer, W. Selecting representative days for capturing the implications of integrating intermittent renewables in generation expansion planning problems. *IEEE Trans. Power Syst.* **2016**, *32.3*, 1936–1948. [[CrossRef](#)]
31. Ludig, S.; Haller, M.; Schmid, E.; Bauer, N. Fluctuating renewables in a long-term climate change mitigation strategy. *Energy* **2011**, *36*, 6674–6685. [[CrossRef](#)]
32. Haydt, G.; Leal, V.; Pina, A.; Silva, C.A. The relevance of the energy resource dynamics in the mid/long-term energy planning models. *Renew. Energy* **2011**, *36*, 3068–3074. [[CrossRef](#)]
33. Teichgraeber, H.; Brandt, A.R. Systematic Comparison of Aggregation Methods for Input Data Time Series Aggregation of Energy Systems Optimization Problems. *Comput. Aided Chem. Eng.* **2018**, *44*, 955–960. [[CrossRef](#)]
34. Teichgraeber, H.; Brandt, A.R. Clustering methods to find representative periods for the optimization of energy systems: An initial framework and comparison. *Appl. Energy* **2019**, *239*, 1283–1293. [[CrossRef](#)]
35. Schütz, T.; Schraven, M.H.; Fuchs, M.; Remmen, P.; Müller, D. Comparison of clustering algorithms for the selection of typical demand days for energy system synthesis. *Renew. Energy* **2018**, *129*, 570–582. [[CrossRef](#)]
36. Baumgärtner, N.; Temme, F.; Bahl, B.; Hennen, M.; Hollermann, D.; Bardow, A. RiSES4 Rigorous Synthesis of Energy Supply Systems with Seasonal Storage by relaxation and time-series aggregation to typical periods. In Proceedings of the ECOS2019—The 32nd International Conference on Efficiency, Cost, Optimization, Simulation and Environmental Impact of Energy Systems, Wroclac, Poland, 23–28 June 2019.
37. Gonzato, S.; Bruninx, K.; Delarue, E. Long term storage in generation expansion planning models with a reduced temporal scope. *Appl. Energy* **2021**, *298*, 117168. [[CrossRef](#)]
38. Gabrielli, P.; Gazzani, M.; Martelli, E.; Mazzotti, M. Optimal design of multi-energy systems with seasonal storage. *Appl. Energy* **2018**, *219*, 408–424. [[CrossRef](#)]
39. Domínguez-Muñoz, F.; Cejudo-López, J.M.; Carrillo-Andrés, A.; Gallardo-Salazar, M. Selection of typical demand days for CHP optimization. *Energy Build.* **2011**, *43*, 3036–3043. [[CrossRef](#)]
40. Kotzur, L.; Markewitz, P.; Robinius, M.; Stolten, D. Time series aggregation for energy system design: Modeling seasonal storage. *Appl. Energy* **2018**, *213*, 123–135. [[CrossRef](#)]
41. Limpens, G.; Moret, S.; Jeanmart, H.; Maréchal, F. EnergyScope TD: A novel open-source model for regional energy systems. *Appl. Energy* **2019**, *255*, 113729. [[CrossRef](#)]
42. Nahmmacher, P.; Schmid, E.; Hirth, L.; Knopf, B. Carpe diem: A novel approach to select representative days for long-term power system modeling. *Energy* **2016**, *112*, 430–442. [[CrossRef](#)]
43. Tso, W.W.; Demirhan, C.D.; Heuberger, C.F.; Powell, J.B.; Pistikopoulos, E.N. A hierarchical clustering decomposition algorithm for optimizing renewable power systems with storage. *Appl. Energy* **2020**, *270*, 115190. [[CrossRef](#)]
44. Pineda, S.; Morales, J.M. Chronological Time-Period Clustering for Optimal Capacity Expansion Planning with Storage. *IEEE Trans. Power Syst.* **2018**, *33*, 7162–7170. [[CrossRef](#)]
45. Teichgraeber, H.; Lindenmeyer, C.P.; Kotzur, L.; Stolten, D.; Robinius, M.; Brandt, A.R. Extreme events in time series aggregation: A case study for optimal residential energy supply systems. *Appl. Energy* **2020**, *275*, 115223. [[CrossRef](#)]
46. Teichgraeber, H.; Küpper, L.E.; Brandt, A.R. Designing reliable future energy systems by iteratively including extreme periods in time-series aggregation. *Appl. Energy* **2021**, *304*, 117696. [[CrossRef](#)]
47. Collins, S.; Deane, P.; Gallachóir, B.O.; Pfenninger, S.; Staffell, I. Impacts of Inter-annual Wind and Solar Variations on the European Power System. *Joule* **2018**, *2*, 2076–2090. [[CrossRef](#)]
48. Kotzur, L.; Markewitz, P.; Robinius, M.; Stolten, D. Impact of different time series aggregation methods on optimal energy system design. *Renew. Energy* **2018**, *117*, 474–487. [[CrossRef](#)]
49. Middelhaue, L.; Ljubic, N.; Granacher, J.; Girardin, L.; Maréchal, F. Data reduction for mixed integer linear programming in complex energy systems. In Proceedings of the ECOS2021—The 34th International Conference on Efficiency, Cost, Optimization, Simulation and Environmental Impact of Energy Systems, Taormina, Italy, 28 June–2 July 2021.
50. Tejada-Arango, D.A.; Domeshek, M.; Wogrin, S.; Centeno, E. Enhanced representative days and system states modeling for energy storage investment analysis. *IEEE Trans. Power Syst.* **2018**, *33*, 6534–6544. [[CrossRef](#)]
51. Hernandez, A.; Thiran, P.; Jeanmart, H.; Limpens, G. EnergyScope Multi-Cell: A Novel Open-Source Model for Multi-Regional Energy Systems and Application to a 3-Cell, Low-Carbon Energy. Master's Thesis, Université Catholique de Louvain, Louvain-la-Neuve, Belgium, 2020.
52. Thiran, P.; Hernandez, A.; Limpens, G.; Moret, S. EnergyScopeMC Repository. Available online: [https://github.com/energyscope/EnergyScope\\_multi\\_cells](https://github.com/energyscope/EnergyScope_multi_cells) (accessed on 10 January 2023).
53. Thiran, P.; Hernandez, A.; Limpens, G.; Moret, S. EnergyScopeMC Documentation 1.3. Available online: <https://energyscope-multi-cells.readthedocs.io/en/master/> (accessed on 10 January 2023).
54. Borasio, M.; Moret, S. Deep decarbonisation of regional energy systems: A novel modelling approach and its application to the Italian energy transition. *Renew. Sustain. Energy Rev.* **2022**, *153*, 111730. [[CrossRef](#)]
55. Muyldermans, B.; Nève, G.; Jeanmart, H.; Limpens, G. Multi-Criteria Optimisation of an Energy System and Application to the Belgian Case. Master's Thesis, Université Catholique de Louvain, Louvain-la-Neuve, Belgium, 2021.

56. Limpens, G.; Coppitters, D.; Rixhon, X.; Contino, F.; Jeanmart, H. The impact of uncertainties on the Belgian energy system: application of the Polynomial Chaos Expansion to the EnergyScope TD model. In Proceedings of the ECOS2020—The 33rd International Conference on Efficiency, Cost, Optimization, Simulation and Environmental Impact of Energy Systems, Osaka, Japan, 29 June–July 3 2020.
57. Limpens, G. Generating Energy Transition Pathways: Application to Belgium. Ph.D. Thesis, Université Catholique de Louvain, Louvain-la-Neuve, Belgium, 2021.
58. Limpens, G.; Jeanmart, H.; Moret, S.; Guidati, G.; Li, X.; Maréchal, F. The role of storage in the Swiss energy transition. In Proceedings of the ECOS2019—The 32nd International Conference on Efficiency, Cost, Optimization, Simulation and Environmental Impact of Energy Systems, Wroclac, Poland, 23–28 June 2019.
59. Limpens, G.; Jeanmart, H.; Maréchal, F. Belgian Energy Transition: What Are the Options? *Energies* **2020**, *13*, 261. [[CrossRef](#)]
60. Colla, M.; Blondeau, J.; Jeanmart, H. Optimal use of lignocellulosic biomass for the energy transition, including the non-energy demand: The case of the Belgian energy system. *Front. Energy Res.* **2022**, *10*, 802327. [[CrossRef](#)]
61. Rixhon, X.; Tonelli, D.; Colla, M.; Verleysen, K.; Limpens, G.; Jeanmart, H.; Contino, F. Integration of non-energy among the end-use demands of bottom-up whole-energy system models. *Front. Energy Res.* **2022**, *10*, 904777. [[CrossRef](#)]
62. Thiran, P.; Hernandez, A.; Limpens, G.; Prina, M.G.; Jeanmart, H.; Contino, F. Flexibility options in a multi-regional whole-energy system: The role of energy carriers in the Italian energy transition. In Proceedings of the ECOS2021—The 34th International Conference on Efficiency, Cost, Optimization, Simulation and Environmental Impact of Energy Systems, Taormina, Italy, 28 June–2 July 2021.
63. Cornet, N.; Eloy, P.; Jeanmart, H.; Limpens, G. Energy Exchanges between Countries for a Future Low-Carbon Western Europe by Merging Cells in EnergyScope MC to Handle Wider Regions. Master's Thesis, Université Catholique de Louvain, Louvain-la-Neuve, Belgium, 2021.
64. Dommissie, J.; Tychon, J.L. Modelling of Low Carbon Energy Systems for 26 European Countries with EnergyScopeTD. Master's Thesis, Université Catholique de Louvain, Louvain-la-Neuve, Belgium, 2020.
65. RTE. *Futurs Energétiques 2050*; Technical Report; RTE: Paris, France, 2022.
66. Dupont, E.; Koppelaar, R.; Jeanmart, H. Global available wind energy with physical and energy return on investment constraints. *Appl. Energy* **2018**, *209*, 322–338. [[CrossRef](#)]
67. Dupont, E.; Koppelaar, R.; Jeanmart, H. Global available solar energy under physical and energy return on investment constraints. *Appl. Energy* **2020**, *257*, 113968. [[CrossRef](#)]
68. European Commission; Directorate-General for Climate Action; Directorate-General for Energy; Directorate-General for Mobility and Transport; Zampara, M.; Obersteiner, M.; Evangelopoulou, S.; De Vita, A.; Winiwarter, W.; Witzke, H.-P.; et al. *EU Reference Scenario 2016: Energy, Transport and GHG Emissions: Trends to 2050*; Publications Office: Luxembourg, 2016. Available online: <https://data.europa.eu/doi/10.2833/001137>.
69. DeCarolis, J.F. Using modeling to generate alternatives (MGA) to expand our thinking on energy futures. *Energy Econ.* **2011**, *33*, 145–152. [[CrossRef](#)]
70. Price, J.; Keppo, I. Modelling to generate alternatives: A technique to explore uncertainty in energy-environment-economy models. *Appl. Energy* **2017**, *195*, 356–369. [[CrossRef](#)]
71. Lombardi, F.; Pickering, B.; Colombo, E.; Pfenninger, S. Policy Decision Support for Renewables Deployment through Spatially Explicit Practically Optimal Alternatives. *Joule* **2020**, *4*, 2185–2207. [[CrossRef](#)]
72. Pickering, B.; Lombardi, F.; Pfenninger, S. Diversity of options to eliminate fossil fuels and reach carbon neutrality across the entire European energy system. *Joule* **2022**, *6*, 1253–1276. [[CrossRef](#)]
73. Dubois, A.; Ernst, D. Computing necessary conditions for near-optimality in capacity expansion planning problems. *Electr. Power Syst. Res.* **2022**, *211*, 108343. [[CrossRef](#)]
74. Grochowicz, A.; van Greevenbroek, K.; Benth, F.E.; Zeyringer, M. Intersecting near-optimal spaces: European power systems with more resilience to weather variability. *Energy Econ.* **2023**, *118*, 106496. [[CrossRef](#)]
75. Neumann, F.; Brown, T. The near-optimal feasible space of a renewable power system model. *Electr. Power Syst. Res.* **2021**, *190*, 106690. [[CrossRef](#)]

**Disclaimer/Publisher's Note:** The statements, opinions and data contained in all publications are solely those of the individual author(s) and contributor(s) and not of MDPI and/or the editor(s). MDPI and/or the editor(s) disclaim responsibility for any injury to people or property resulting from any ideas, methods, instructions or products referred to in the content.